Available online at www.sciencedirect.com
SCIENCE DIRECT®
Journal of volcanology and geothermal research
Journal of Volcanology and Geothermal Research 154 (2006) 317–324
www.elsevier.com/locate/jvolgeores

Short communication

Origins and implications of zigzag rift patterns on lava lakes

Leif Karlstrom [a], Michael Manga [b,*]

[a] Department of Physics, University of Oregon, Eugene, OR 97403, USA
[b] Department of Earth and Planetary Science, University of California, Berkeley, CA 94720, USA

Received 7 September 2005; received in revised form 18 January 2006; accepted 30 January 2006
Available online 23 March 2006

Abstract

The distinctive rift patterns observed on newly formed lava lakes are very likely a product of interaction between heat transfer (cooling of lava) and deformation of the solid crust in response to applied stresses. One common pattern consists of symmetric "zigzag" rifts separating spreading plates. Zigzags can be characterized by two measurable parameters: an amplitude A, and an angle θ between segments that make up the zigzags. Similar patterns are observed in analog wax experiments in which molten wax acts as cooling and solidifying lava. We perform a series of these wax experiments to find the relationship between θ, A, and the cooling rate. We develop a model to explain the observed relationships: θ is determined by a balance of spreading and solidification speeds; the amplitude A is limited by the thickness of the solid wax crust. Theoretical predictions agree well with experimental data; this enables us to scale the model to basaltic lava lakes. If zigzag rifts are observed on the surface of lava lakes, and if physical properties of the lava crust can be measured or inferred by other means, measurements of θ and A make it possible to calculate crust-spreading velocity and crust thickness.

Keywords: lava lakes; rifting; solidification; pattern formation

1. Introduction

The surface of lava lakes consists of rigid plates separated by rifts filled with hotter, fluid magma. The pattern and dynamics of these plates on lava lakes has been used to better understand several geological processes. For example, the evolution of surface patterns and the velocity of plates can be used to study convective regimes in the interior of the lava lake (e.g., Harris et al., 2005). Because cooling causes solidification and hence a change in rheology from liquid-like to solid-like, the interaction of the plates on the surface of lava lakes has also served as a model for global plate tectonics (e.g., Duffield, 1972). Finally, patterns on terrestrial lava lakes provide a template for interpreting surfaces features on Jupiter's moon Io (e.g., Radebaugh et al., 2004).

Often the rifts make distinctive patterns, forming jagged lines at an angle to the direction of crustal spreading. Fig. 1 shows one common pattern: a "zigzag" rift in which the rift width is constant, and the angle with a line perpendicular to the spreading direction is the same for every kink in the rift. If we know the mechanism that makes zigzag rifting patterns, we can estimate the physical features of the newly formed crust, and therefore gain a better understanding of the geological processes at work.

Ragnarsson et al. (1996) observed similar rifting patterns in an investigation of spreading wax layers. Fig.

* Corresponding author. Fax: +1 510 643 9980.
E-mail addresses: lkarlstr@gladstone.uoregon.edu (L. Karlstrom), manga@seismo.berkeley.edu (M. Manga).

0377-0273/$ - see front matter © 2006 Elsevier B.V. All rights reserved.
doi:10.1016/j.jvolgeores.2006.01.004

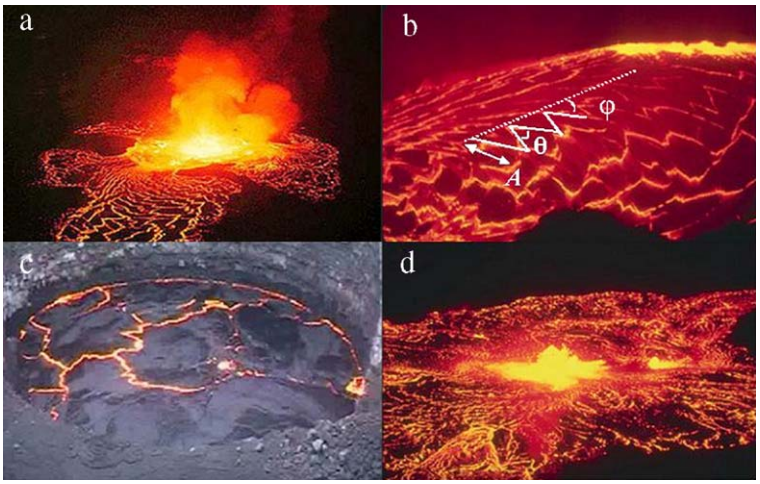

Fig. 1. Photographs of active lava lakes display the common zigzag rift pattern. Fountains are usually regions of crust subduction. (a) Lava lake on Nyiragongo, Democratic Republic of the Congo, 1994. Photo by Jack Lockwood, U.S.G.S. (b) Mauna Ulu lava lake, Hawaii, 1972. Photo by R.T. Holcomb, Hawaiian Volcano Observatory, U.S.G.S. Amplitude A and angles θ and φ are indicated. (c) Erta Ale lake, Ethiopia, 2002. Photo by J. Alean, R. Carniel, and M. Fulle at http://www.Stromboli.net. (d) Kilauea summit lava lake, Hawaii, 1967. Photo by C. Stoughton, Hawaiian Volcano Observatory, U.S.G.S.

2 shows the three regimes of rift geometries found in their experiments, corresponding to different ranges of crustal-spreading velocities. The zigzag regime exhibits the same properties – constant width, characteristic angle – as that on lava lakes. They found that, for spreading velocities that resulted in zigzags (Fig. 2b), the characteristic angle $\varphi=(90°-\theta/2)$ (indicated in Fig. 1b) was constant for a given pulling speed, and obeyed the geometrical relation

$$\cos(\varphi)=\frac{v_g}{v_p}, \tag{1}$$

where v_p is the crust-spreading speed and v_g is the crust growth speed. φ approached 90° as the spreading rate increased, at which point the rift developed transform-type faults parallel to the spreading direction, separated by straight segments nearly perpendicular to the transform boundaries (Fig. 2c).

Here we present the results of an experimental study, using solidifying molten wax as an analogue for the lava lake, in order to understand the origins of the zigzag pattern and the processes that control the features of the rift. We find that the two characteristic features of these rifts – the angle φ and the amplitude A (Fig. 1b) – depend on the spreading speed and the cooling rate (controlled by the wind speed). We develop a theoretical model that can explain the experimental observations and can thus be scaled to lava lakes. This model will then be shown to agree with observations.

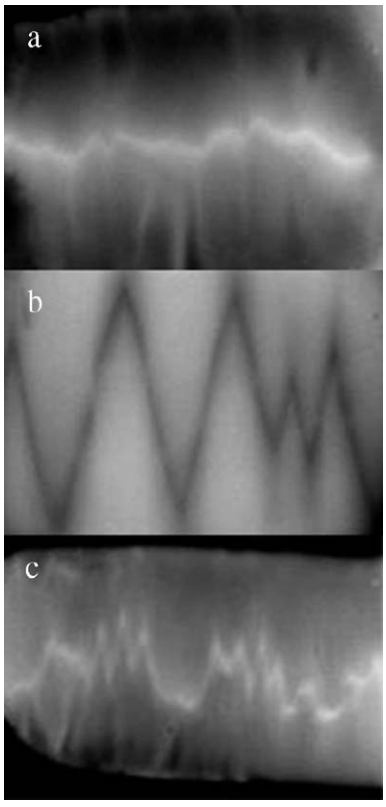

Fig. 2. Infrared images of three rifting regimes in paraffin wax experiments: (a) Slow spreading speeds (v_p=230 μm/s). White is hot. (b) "Zigzag" regime of rift formation in wax (v_p=414 μm/s). Black is hot. (c) Fault-like regime of rift formation in wax (v_p=535 μm/s). White is hot.

2. Experiment

We use a commercial macrocrystalline paraffin wax with melting point of 53 °C as an analog for basaltic magma because previous studies have shown that the surface features on both solidifying wax and lava are governed by the interaction between deformation and heat transport, and hence that it is possible to scale from analog wax experiments to lavas (Oldenburg and Brune, 1972; Mancktelow, 1988, Rossetti et al., 1999; Griffiths, 2000 – rheological properties of similar wax are reported in Rossetti et al., 1999). Our experimental setup, shown in Fig. 3, is adapted from the one used in Manga and Sinton (2004). We heat a $20\times20\times5\,\mathrm{cm}^3$ container of wax from the bottom with a variable resistance heater. Once the wax is completely molten, fans placed at each corner of the container are turned on, cooling the surface of the wax until a uniform layer of solid crust forms, usually from 0.5 to 1 cm in thickness, which is measured by making an incision in the solid crust. We found that the initial thickness of the crust does not affect the rifting pattern. This is because once a rift forms, it is the newly solidified wax that governs the ongoing morphological changes in the surface; the original layer only acts as an anchor for the new crust.

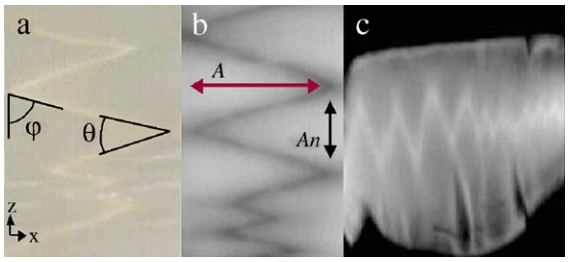

Fig. 4. (a) Optical image of zigzag rift, with the angles φ and θ defined. (b) Infrared image of zigzag rift, with the amplitude A, and normal A_n drawn in. (c) Infrared image demonstrating the effect of wind speed on pattern amplitude. The wind speed is higher on the right side of the picture.

To initiate a rift, the solid wax crust is slit with a razor blade the length of the container, parallel to the paddle, and then the motor is turned on. The wax crust is then pulled apart uniformly for the length of the container, a process lasting 6–10 min, while the heat flux supplied from below, and the cooling rate from above, remain constant.

We calculate the constant pulling speed v_p by dividing the total displacement of the paddle by the duration of the experiment. Features of the pattern, the angle θ and the amplitude A, are recorded by a 5.5 megapixel CCD camera and by an infrared 8–

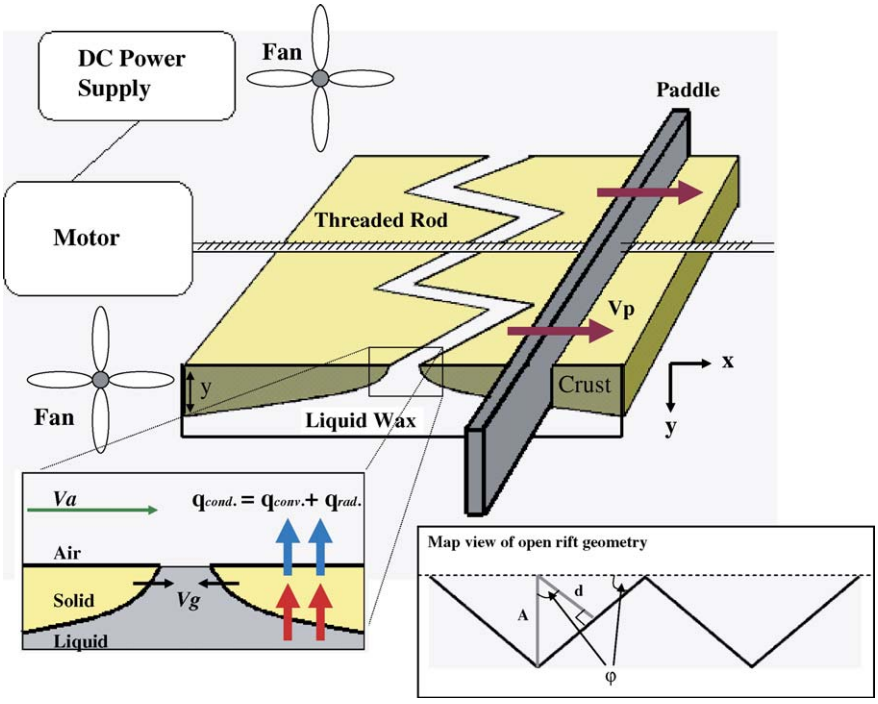

Fig. 3. Schematic illustration of the experimental apparatus. Left inset: Local heat transfer mechanisms, wind speed v_a and growth velocity v_g. Right inset: Rift geometry (zigzags represent open rift segments), and the parameters A, d, and φ.

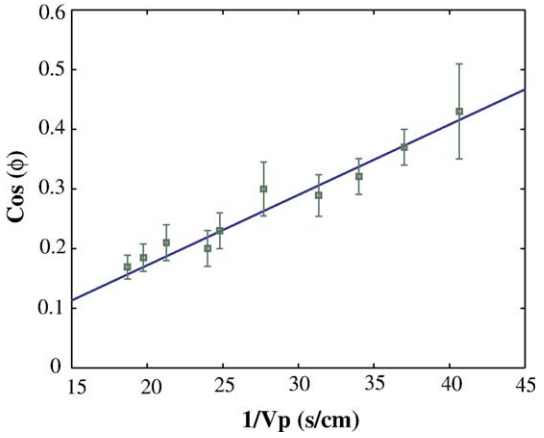

Fig. 5. Model, Eq. (1), compared with data at constant wind speed.

16 micron wavelength camera (160 × 120 pixel JTL1 Infrared Imager), to digital files. The infrared images are preferable for analysis, because the presence of other optical light sources does not affect the image quality (Fig. 4).

Observed features are then measured with the NIH ImageJ software, which allows a pixel-level analysis of angles and distances. To measure an angle, we draw lines over an infrared image, and calculate the angle θ. Since there is some error associated with visually finding the darkest (or lightest) pixels of a given feature, we measure 10–15 angles in each figure and average them. This averaged value of θ and its uncertainty are then used in calculating the characteristic angle φ of the rift according to

$$\varphi = (180-\theta)/2. \quad (2)$$

Amplitudes are defined as the distance from the apex of the rift pattern to a normal line connected the two adjacent apexes (Fig. 4b). Amplitudes are calculated by drawing in the normal line A_n, counting the pixels, and scaling the pixel size to an actual distance. Then we use the formula:

$$A = (A_n/2)/\tan[\theta/2] \quad (3)$$

The characteristic amplitude of the rift A is the average of 10–15 such calculations. The standard deviation of A is calculated with the uncertainties in A_n, and in θ.

Another measured variable in our experiments is the wind speed, which is controlled by placing a fan so that it is blowing across the rift, then adjusting its power and distance from the container to vary wind speed over the wax. We measure this quantity with a Hotwire Anemometer (Eurotron Mini Air HW PRO-VT50), placed above the hydrodynamic boundary layer of the container, to measure the free stream velocity. Since the flow is forced-turbulent, we use a wind speed averaged over 30 s. Error is estimated by repeating the measurements.

We carry out two sequences of experiments, varying crustal-spreading speed v_p and wind speed v_a systematically to determine the resulting behavior of features φ and A. Although we confirm the previous result of varying v_p (Fig. 5), we find a previously overlooked dependence of φ on wind speed (Fig. 6), as well as a systematic relation between A and v_a (Fig. 4c). The interpretation of these results is discussed next.

3. Model

A scalable description of the zigzag rift pattern in wax must account for the dependence of its measurable quantities, φ and A, on external influences such as the cooling rate, as well as the internal temperature differences that drive solidification. We would like to calculate the thickness of the newly forming solid layer, and also calculate quantities such as the surface temperature of the crust T_s, and growth velocity v_g, which may be difficult to measure. Doing this, we can proceed to a scaled model for lava.

In the study of Ragnarsson et al. (1996), rifts in the zigzag regime were found experimentally to obey Eq. (1), where v_g is the growth rate in the x–z plane (indicated in Fig. 3). They infer that v_g is constant from the observation of constant rift width, under the assumption that constant width is caused by a constant temperature at the wax–air interface, a constant latent heat release, and constant growth velocity perpendicular to a rift front. However, this relation holds only when the wind speed v_a is constant. Since we expect that wind

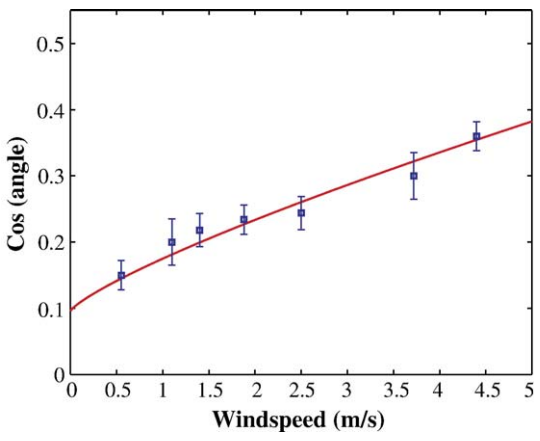

Fig. 6. Relation between φ and v_a compared with model, Eq. (7).

speed controls v_g, we extend the scaling of Eq. (1) to include a variable cooling rate.

Given that the temperature gradient is much greater in the vertical than horizontal direction, we construct a local energy balance, in which the vertical conductive heat flux through solidifying crust is balanced by convective and radiative heat loss to the overlying air, similar to other approaches to local heat transfer in lavas (e.g., Neri, 1997):

$$\frac{k(T_l-T_s)\sqrt{v_p}}{\mathrm{erf}\lambda\sqrt{\kappa\pi x}} = \varepsilon\sigma(T_s^4-T_a^4) + h(T_s-T_a). \quad (4)$$

The left side of Eq. (4) represents a solution to the Stefan Problem, a common model for the top-down cooling and solidification of a fluid layer. It is a similarity solution to the Fourier heat conduction equation, in which a half space is cooled from above, and solidification occurs from the top surface down. The position of the solidification boundary in the vertical direction, denoted by the dimensionless coordinate λ, is a function of the square root of time, and may be found solving the diffusion problem within the solid crust accounting for latent heat release at the lower boundary (for a full derivation of the solution to the Stefan Problem, see for example Turcotte and Schubert, 2002, pp. 162–166). At any point in time, λ is a constant, given by the implicit equation

$$\frac{L\kappa\rho k\sqrt{\pi}}{c(T_l-T_s)} = \frac{e^{-\lambda^2}}{\lambda\mathrm{erf}\lambda} \quad (5)$$

In Eqs. (4) and (5), κ is the thermal diffusivity, k is the thermal conductivity, L is the latent heat of solidification, ρ is the density, T_l is the liquid temperature, T_s is the surface temperature, and T_a is the mean free stream temperature of the air. The two terms on the right side of Eq. (4) describe radiative and convective heat loss to the air, respectively. Here $\varepsilon=1$ is the emissivity, and σ is the Stefan–Boltzman constant. Although the radiative heat flux will far outweigh the convective term for most studies of cooling lava (e.g., Keszthelyi et al., 2003), convective heat loss is the dominant mechanism for our wax experiments. We use a turbulent-flow estimation of the heat transfer coefficient h for air over a flat plate (a dimensionalized Stanton number, Holman, 2002, p. 237, Eqs. (5)–(81)),

$$h = \frac{\beta Re^{-1/5}\rho c v_a}{Pr^{2/3}}, \quad (6)$$

where $\beta=0.0204$ is our experimentally determined empirical constant, Re (proportional to v_a) is the Reynolds number, Pr is the Prandtl number, and c is the specific heat capacity.

We assume that the growth rate of the wax v_g in the x–z plane (Fig. 3) is proportional to the temperature difference across the solid layer T_l-T_s. This is justified by an implicit calculation (using a rearrangement of Eq. (4)) of the surface temperature in the vicinity of the rift. We find that it varies by less than 2 °C over a few mm, and therefore infer that a nearly constant temperature will imply a nearly constant horizontal growth rate in the vicinity of the rift. Hence, φ obeys

$$\cos(\varphi) = \frac{\alpha(T_l-T_s)}{v_p} = \frac{\alpha\mathrm{erf}\lambda\sqrt{\kappa t\pi}}{v_p k}[\varepsilon\sigma(T_s^4-T_a^4) + h(T_s-T_a)], \quad (7)$$

where $\alpha=3.6\times10^{-5}$ is the experimentally determined constant of proportionality. When Eq. (7) is compared to Eq. (1), v_g is seen to have a strong dependence on wind speed, when convective heat loss is comparable to radiation. x/v_p is replaced with t here because we interested in the growth rate evaluated after a particular time. In Eq. (7), T_s is calculated directly from Eq. (4), and it is approximately constant over distance of several millimeters in the horizontal direction away from the rift.

To find a relation for A, we examine the evolution of the rift pattern from the initial incision to the final constant-amplitude zigzags. At the onset of the pattern, small zigzags are not stable – they collapse upon each other and grow together to form larger zigzags (see Ragnarsson et al. (1996) for illustration of this growth). φ, however, remains constant as the amplitude of the rifts increases. The eventual existence of a stable pattern size in our experiments, for a given characteristic angle φ, suggests that there is a critical thickness of wax crust beyond which the zigzag pattern will no longer propagate. This thickness should be independent of the crust-spreading speed and constant for all v_p. It should involve a balance of zigzag growth in the horizontal plane, and crustal thickening in the vertical direction. This may be made more explicit by examining the characteristic rift angle φ. As φ grows larger, the perpendicular distance from the rift, d (see Fig. 3), to the line behind the apex of the rift that defines the amplitude of the pattern shrinks as $\cos(\varphi)$. Advection of new wax will likely occur at the same rate perpendicular to the rift as well as parallel to the direction of spreading speed (Eq. (9)), but zigzag coalescence, and therefore the position of a critical wax thickness in the final stable pattern depends on the rift angle. In this way, as φ

grows, the critical thickness of wax η will occur closer to the apex of the rift according to

$$y\cos(\varphi) = \eta, \tag{8}$$

evaluated at amplitude A. Then, since

$$y(A) = 2\lambda\sqrt{\frac{\kappa d}{v_p\cos(\varphi)}} = 2\lambda\sqrt{\frac{\kappa A}{v_p}} \tag{9}$$

from the Stefan problem (Turcotte and Schubert, 2002), we can solve for A, to obtain

$$A = \frac{v_p}{\kappa}\left(\frac{\eta}{2\lambda\cos(\varphi)}\right)^2, \tag{10}$$

an explicit expression for amplitude.

The model (Eqs. (7), (8) and (10)) can be compared with the experimental data. Table 1 shows values for wax. We find that the characteristic angle φ is highly variable with respect to pulling speed and wind speed. We confirm the suitability of the geometrical model, Eq. (1), of Ragnarsson et al. (1996) for constant wind speed (Fig. 5), and calculate a growth velocity v_g of 118 μm/s for the zigzag regime, with v_p in the range of 250–500 μm/s. We find that φ has a nearly linear dependence on wind speed (Fig. 6). Eq. (7) explains the slight curvature: for systems in which convective heat transfer is significant, φ varies as $v_a^{4/5}$. For lava lakes, radiation is expected to dominate the heat transfer (Keszthelyi et al., 2003), and so wind speed dependence of φ should be negligible.

It is also clear that varying the wind speed changes the pattern-regime of rifting, in similar ways as in Fig. 2, thereby affecting the amplitude A of the pattern. When wind speed is too low, the rift exhibits fault-like boundaries interspersed with regions of liquid wax. When wind speed is too high, the rift maintains the shape of the initial incision, and zigzags do not form. We find for the region in which zigzags occur that Eq. (10) fits data taken at two constant pulling speeds (Fig. 7). The amplitudes of rift patterns have therefore a strong dependence on pulling speed and wind speed.

The critical thickness of the wax limiting rift propagation, however, does not depend on wind speed (Fig. 8). We find from Eq. (8) that $\eta = 2.3 \pm 0.3$ mm for the measured pulling speeds. Thus, we conclude that for rifting systems, there will be a characteristic crust thickness (presumably material-dependent) at which patterns can no longer grow.

Table 1
Physical properties of wax and lava

Quantity	Paraffin wax	Basaltic lava
Density, ρ	600 kg/m^3 [a]	3000 kg/m^3 [b]
Diffusivity, κ	9×10^{-8} m^2/s [c]	7×10^{-6} m^2/s
Thermal conductivity, k	0.24 W/mK [c]	3 W/mK [b]
Latent heat of solidification, L	200 kJ/kg [d]	400 kJ/kg [e]
Specific heat, c	2.9 kJ/kg [c]	1 kJ/kg [e]
Liquid temperature, T_l	325 K [a]	1415 K [b]
Air temperature, T_a	298 K [a]	298 K [f]
Stefan constant, λ	1.83 [a]	0.876 [e]

[a] Measured by authors.
[b] Representative early time value.
[c] From Goodhew and Griffiths (2003).
[d] From Ragnarsson et al. (1996).
[e] From Turcotte and Schubert (2002).
[f] Estimated.

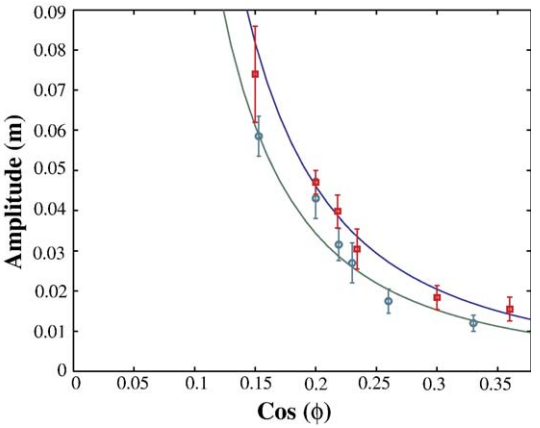

Fig. 7. Data compared with model predictions for v_p=420 μm/s (red squares) and v_p=300 μm/s (green circles) using Eq. (10) (wind speed varies implicitly).

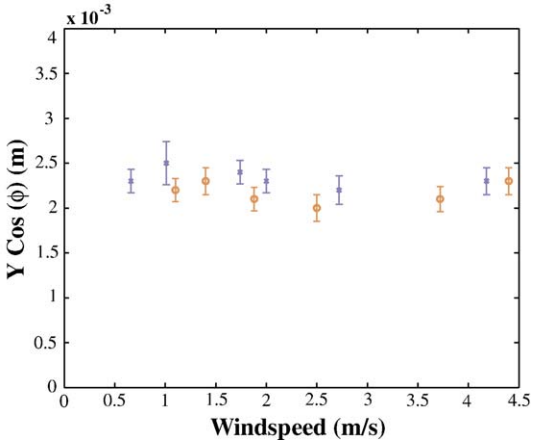

Fig. 8. Wind speed versus thickness of wax at amplitude A for v_p=420 μm/s (blue x's) and v_p=300 μm/s (orange o's) obtained using Eq. (8). (For interpretation of the references to colour in this figure legend, the reader is referred to the web version of this article.)

4. Scaling to lava lakes, and other implications

Basaltic lava lakes, and lava flows on which there is newly forming crust, can exhibit the same rifting regimes as the analog wax system. As is evident from footage taken at active lava lakes (e.g. from Erta Ale, by J. Alean, R. Carniel, M. Fulle at http://www.stromboli.net), an actively resurfacing lake on which the crust spreads at varying speeds goes through all regimes of rift formation. If it is possible, then, to associate an observed crust-spreading speed with the zigzag rift formation, our model makes it possible to determine the critical thickness of the crust. Likewise, if the crust thickness can be measured, or calculated by other means, a spreading speed may be calculated, as an alternative to other methods (e.g., Harris et al., 2005), by measuring the amplitude A, the angle θ of the pattern, and then using Eq. (10).

To test the validity of our model on lava lakes, we use data gathered by Harris et al. (2005) from the active lake of Erta Ale, and representative values for the relevant physical quantities (see Table 1). Using an infrared thermal time series, Harris et al. measured crust velocities in the range of 3.6–37.8 cm/s for highly active periods of resurfacing, when the zigzag regime of rift patterns is common. From the digital footage taken during those periods, and with a correction for the oblique viewing angles of the photos, we estimate values of φ in the range of 45°–65°, and values of A in the range of 3–15 m. Therefore, we expect the limiting thickness of crust for lava lakes in the regions experiencing active resurfacing to be in the range of 1–15 cm. This estimate is of the same magnitude as other crust-thickness models based on energy balance methods (e.g., Hon et al., 1994), that report crust thickness values in the same range as ours. It represents the thickness of crust that has sufficient strength to prevent the rifts from propagating. If we are able to determine the yield strength of this crust, e.g., through lab experiments (e.g., Hoover et al., 2001) or through field measurements, we can perhaps obtain an estimate of the stresses exerted by the convecting lava on the crust, and hence further insight into lava lake convection. Because the scaling procedure used for lava lakes appears to agree well with our experiments, it provides a basis for interpreting rift patterns both on Earth and other planets. If the physical properties of the magma on the surface of Io, for example, can be determined, crust thickness, and therefore resurfacing rates may be found with images of high enough resolution to identify rift patterns.

The model developed here has other applications as well. Similar processes may operate in lava flows, where crust formation may be responsible for the morphological transition between pahoehoe and a‘a‘ basaltic lava flows (Fink and Griffiths, 1992). Because the formation of a‘a‘ flows probably depends on a high rifting rate of newly formed crust (Kilburn, 2003), we infer that the critical thickness of crust in the zigzag regime could be similar to the crust thickness required to form a‘a‘ flows.

Acknowledgements

We thank Lockheed Martin for the use of the infrared camera, NASA grants NNG05GA25G, NNG04GE89G and NSF Grant No. EAR0439766 for financial support. We also thank Atsuko Namiki, Ikuro Sumita and two reviewers (Ross Kerr and an anonymous reviewer) for their constructive comments on the project and manuscript.

References

Duffield, W.A., 1972. Naturally occurring model of global plate tectonics. Journal of Geophysical Research 17, 2543–2555.

Fink, J.H., Griffiths, R.W., 1992. A laboratory analog study of the surface morphology of lava flows extruded from point and line sources. Journal of Volcanology and Geothermal Research 54, 19–32.

Goodhew, S., Griffiths, R., 2003. Analysis of thermal-probe measurements using an iterative method to give sample conductivity and diffusivity data. Applied Energy 77, 205–223.

Griffiths, R.W., 2000. The dynamics of lava flows. Annual Review of Fluid Mechanics 32, 477–518.

Harris, A.G.L., Carniel, R., Jones, J., 2005. Identification of variable convective regimes at Erta Ale lava lake. Journal of Volcanology and Geothermal Research 142, 207–223.

Holman, J.P., 2002. Heat Transfer. McGraw-Hill, New York.

Hon, K., Kauahikaua, J., Denlinger, R., Mackay, K., 1994. Emplacement and inflation of Pahoehoe sheet flows – observations and measurements of active lava flows on Kilauea volcano, Hawaii. Geological Society of America Bulletin 106, 351–370.

Hoover, S.R., Cashman, K.V., Manga, M., 2001. The yield strength of subliquidus basalts – experimental results. Journal of Volcanology and Geothermal Research 107, 1–18.

Keszthelyi, L., Harris, A.J.L., Dehn, J., 2003. Observation of the effect of wind on the cooling of active lava flows. Geophysical Research 30, doi:10.1029/2003GL017994 (art. no. 1989).

Kilburn, C.R.J., 2003. Fracturing as a quantitative indicator of lava flow dynamics. Journal of Volcanology and Geothermal Research 132, 209–224.

Mancktelow, N.S., 1988. The rheology of paraffin wax and its usefulness as an analog for rocks. Bulletin of the Geological Institutions of the University of Uppsala, N.S. 14, 181–193.

Manga, M., Sinton, A., 2004. Formation of bands and ridges on Europa by cyclic deformation: insights from analog wax experiments. Journal of Geophysical Research E090001, doi:10.1029/2004JE002249.

Neri, A., 1997. A local heat transfer analysis of lava cooling in the atmosphere: application to thermal-diffusion dominated flows. Journal of Volcanology and Geothermal Research 81, 215–243.

Oldenburg, G.W., Brune, J.N., 1972. An explanation for the orthogonality of ocean ridges and transform faults. Journal of Geophysical Research 80, 2575–2585.

Radebaugh, J., McEwen, A.S., Milazzo, M.P., et al., 2004. Observations and temperatures of Io's Pele Patera from Cassini and Galilee spacecraft images. Icarus 169, 65–79.

Ragnarsson, R., Ford, J.L., Santangelo, C.D., Bodenshatz, E., 1996. Rifts in spreading wax layers. Physical Review Letters 76, 3456–3459.

Rossetti, F., Ranalli, G., Faccenna, C., 1999. Rheological properties of paraffin as an analog material for viscous crustal deformation. Journal of Structural Geology 21, 413–417.

Turcotte, G.L., Schubert, G., 2002. Geodynamics. Cambridge University Press, New York.